Chapter

Preparation, Characterization, and Swelling Behavior of PEGylated Guar Gum @ Ag Nanoparticles

Selcan Karakus, Ezgi Tan, Merve Ilgar, Ibrahim Mizan Kahyaoglu, Yeşim Müge Şahin, Demet Sezgin Mansuroglu, Deniz Ismik, Nevin Tasaltin and Ayben Kilislioglu

Abstract

In this study, polyethylene glycol/guar gum @ silver nanoparticles (PEG/GG@AgNPs) were synthesized by using simple sonication method. The nanoparticles were characterized using Fourier-transform infrared spectroscopy (FTIR) and scanning transmission electron microscopy (STEM). The swelling behaviors of nanoparticles were studied in different pHs (5.5 and 7.4). The experimental results were calculated by Fickian diffusion and Schott kinetic models to understand the swelling mechanism and coefficients of the nanoparticles. The results showed that the linear equation of the Fickian diffusion kinetic model was best fit to explain the water diffusion mechanism of the nanoparticle with high correlation coefficient (R^2 = 0.982–0.987). The results confirmed that the swelling degree of nanoparticles were 9.71 g/g at pH 5.5. Also, the results confirmed that PEG/GG@AgNPs can be a good candidate for drug delivery systems in pharmaceutical applications.

Keywords: swelling behavior, guar gum, Ag nanoparticles

1. Introduction

Nanotechnology focuses on many fundamental disciplines such as physics, chemistry, materials science, and biology [1]. Recently, the synthesis of the nanostructures has gained a great attention due to superior properties (mechanical, optical, thermal, biological, physical, and chemical) as compared to conventional materials [2–5].These superior properties depend on the size, composition, shape, and origin of nanostructures [6, 7]. As a general definition, nanostructures are 1–100 nanometers in size in which case they have a high surface area-to-volume ratios and their reactivities are effected mostly depending on their different shapes such as spherical, conical, spiral, cylindrical, tubular, and hollow [8, 9].

Many researchers have reported that iron [10], copper [11], gold [2], and silver [12] were used often for the preparation of stable dispersions of nanoparticles due to their biocompatibility and biodegradability and less reactivity in the biomedical applications. Silver nanoparticles (AgNPs) with desired morphologies, well-known for their antimicrobial activity, are used in both ionic and metallic forms which are incorporated inside the polymer matrix, with excellent biocompatibility [13]. It was known that bare silver nanoparticles were prone to oxidation and tarnishing. Thus, we used PEG/GG polymer blends to improve the dispersion stability and prevent agglomeration of silver nanoparticles in aqueous environment [14].

During the preparation of hydrogels, mostly preferred biopolymers are alginate, chitosan, gum arabic, agar, carrageenans, and guar gum [15–19]. Among these biopolymers, GG is used in the fields of food industry and pharmaceutical and cosmetic applications [20–22]. It is not desirable to prepare silver nanoparticles by chemical methods using toxicological chemicals such as reducing agents [23]. For this purpose, we chose a dual biopolymer blend (GG and PEG) which will carry out the green synthesis and improve the distribution. GG is a nonionic water-soluble polysaccharide and consists of galactomannan which has a linear chain of (1-4)-β-D-mannopyranosyl units interposed with (1-6)-α-D-galactopyranosyl units distributed as side branches [24]. PEG is a stabilizer effective for the control of size and shape of nanoparticles and also has role on the reduction of silver ions [25].

The key points of the chapter were (i) the green synthesis and (ii) swelling of nanoparticles. The aim of this study was to obtain NPs consisting of PEG/GG and zero valent Ag by using the simple sonication method. We prepared nanoparticles in the presence of silver nitrate in GG/PEG (2:1 mixing ratio) polymer blends. In particular, we performed a green synthesis sonochemical process to reduce Ag ions to form AgNPs by using ultrasonic method without the use of dangerous stabilizing agents such as any reducing agent and surfactant [26]. The breaking of cavitation bubbles under high temperature and pressure and the hydrogen radicals (H^*) and hydroxyl radicals (OH^*) in the water formed by the ultrasonic effect play an important role in the reduction of Ag ions and the formation of AgNPs [27].

All samples were characterized by using FTIR and STEM techniques. SEM images revealed good compatibility and homogeneous distribution between the PEG/GG matrix and Ag. AgNPs were found to be <500 nm in size. Moreover, we have also demonstrated the swelling behavior of the prepared nanoparticles in finding out the potential of the nanoparticles for drug delivery systems. The swelling uptake (%) of PEG/GG@AgNPs was found to be % 670.5 at pH 5.5.We determined the swelling behavior such as the maximum swelling and gel fraction of samples to interpret the water absorption results. All results showed that one could control the size and the shape of zero valent Ag nanoparticles by polymer blend under the sonication effect.

2. Materials and methods

2.1 Materials

Guar gum (99% purity, average molecular weight of 2.8×10^5 g mol^{-1}) and polyethylene glycol (PEG 400) were obtained from Fluka (Switzerland). Silver nitrate ($AgNO_3$), sodium hydroxide (NaOH), and dimethyl sulfoxide (DMSO) were obtained from Merck (Pvt.) Ltd. Mumbai, India. Polyethylene glycol 400 (PEG) (molecular weight of 400 g/mol) was purchased from Sigma-Aldrich, Chemie GmbH, USA.

2.2 Preparation of nanoparticles

2.2.1 Preparation of PEG/GG@AgNPs

GG solution (0.5 g GG in 100 mL of deionized water) and PEG (5 mL) were mixed by stirring with a magnetic stirrer at 25°C for 10 min. 5 mL of $AgNO_3$ (0.1 M) solution was added into GG/PEG solutions and then was sonicated for 15 min. 0.1 M NaOH was added into the solutions until pH 8.4.

2.3 Characterization

Samples were ground with KBr powder and analyzed from 4000 to 600 cm^{-1} with a resolution of 4 cm^{-1} using eight scans by using a PerkinElmer FTIR emission spectrometer (Spectrum Two). Samples were scanned in the dark-field area with the wet STEM detector by using FEI QUANTA S50 (A copper grid, Ted Pella, support films, carbon type A, 300 meshes was utilized). STEM holder was cooled to 2°C and the pressure was set between 700 and 1300 Pa.

2.4 Swelling studies

2.4.1 Measurement of the water absorbency

The swelling degree (St, g/g) was calculated from Eq. (2):

$$S_t = \frac{W_t - W_d}{W_d} \tag{1}$$

where S_W is the swelling degree per gram dried sample (g g^{-1}), W_d is the mass of dried samples at time t (g), and W_t is the mass of swollen samples at time t (g) [28].

2.4.2 Calculations of the swelling behavior

The swelling behavior was explained by applying different kinetic models such as Fickian diffusion and Schott second-order dynamic model given in Eqs. (2)–(7) [29, 30]. To identify the swelling kinetic mechanisms of the prepared samples, the swelling kinetic parameters were evaluated according to models:

Fickian diffusion swelling kinetic models:

$$S_t = S_\infty x\left(1 - e^{-k_W t}\right) \tag{2}$$

When Eq. (2) was linearized

$$Ln\frac{S_t}{S_\infty} = Lnk + nLnt \tag{3}$$

where t is time (min), k is the rate constant (min^{-1}), St is the water absorption capacity at time t, and S_∞ is the water absorption capacity at equilibrium. The plots of $Ln S_t/S_\infty$ versus Ln t were drawn to calculate the parameter (k) of kinetic model and the linear correlation coefficient.

Schott proposed the second-order kinetic model to elucidate the swelling mechanism of the system, and this model was related to the swelling rate at any time and

was proportional to the quadratic of the swelling capacity before the equilibrium state [30, 31]:

$$\frac{dS}{dt} = k_s(S_t - S_\infty)^2 \tag{4}$$

When the initial condition was t = 0 and S = 0

$$\frac{t}{S} = A + Bt \tag{5}$$

$$A = 1/k_s S_\infty^2 \tag{6}$$

where t is time (min), S is the swelling capacity at time t (g g^{-1}), A is the reciprocal of initial swelling rate, and B is the reciprocal of S_∞. The plots of t/W versus t were drawn to calculate the parameters (A and B) of kinetic model and the linear correlation coefficient.

To explain the water diffusion mechanism, fractional solution capacity (F: S_t/ S_∞) less than 0.60 was analyzed using the following equation (Eq. (7)):

$$\frac{S_t}{S_\infty} = kt^n \text{ or } \quad F = kt^n \tag{7}$$

where t is time (min), Wt is the uptake capacity of the sample at time t, S_∞ is the capacity of the sample at swelling equilibrium (g), k is the gel characteristic constant, and n is the swelling index (n < 0.5 for Fickian diffusion and 0.5 < n < 1 for non-Fickian; n = 1 for relaxation controlled transport and n > 1 for II diffusion) [30].

The Fickian diffusion model had another expression shown as Eq. (8):

$$\frac{S_t}{S_\infty} = 4\sqrt{\left(D/\pi l^2\right)}\left[\frac{1}{\pi^2} + 2\sum_{n=1}^{x}(-1)^n ierfc\left(\frac{nl}{2\sqrt{Dt}}\right)\right] \tag{8}$$

Diffusion coefficient D (cm^2/s) was calculated using Eq. (9). For short times, Eq. (9) was used at the early-stage diffusion coefficient of water by

$$\frac{S_t}{S_\infty} = 4\sqrt{\left(D/\pi l^2\right)} \tag{9}$$

where l was the diffusional distance [32, 33].

3. Results and discussions

3.1 Swelling kinetics

Swelling ability is known to be associated with free hydrophilic groups and surface properties [34]. The sonication method, which is associated with various factors such as ultrasound power, ultrasound frequency, modification time, and temperature, changes the surface properties [35]. In this study, the swelling kinetics was investigated to determine the surface properties of the novel PEG/GG@AgNPs obtained by using sonication method. To analyze the effect of sonication on the swelling kinetic mechanism of the synthesized nanoparticles, swelling kinetic results were observed gravimetrically and performed in pH 5.5 and 7.4 at 25°C.

The equilibrium swelling degrees, Fickian and Schott kinetic models of PEG/GG@AgNPs were given in **Figures 1–3**, respectively and the swelling behavior followed a similar behavior due the high surface area.

The O-H groups of the PEG/GG@AgNPs formed hydrogen bonds with water molecules and absorbed water [36]. The equilibrium swelling degrees of PEG/GG@AgNPs were 9.71 gg^{-1} (pH 5.5) and 3.82 gg^{-1} (pH 7.4). According to the experimental swelling results, the swelling degree of the PEG/GG@AgNPs increased within the first 10 minutes and then slowed down until reaching equilibrium after 15 min in two different pH mediums. In this case, the results showed that the nanoparticle had shown greater interest in the water molecules and was proof

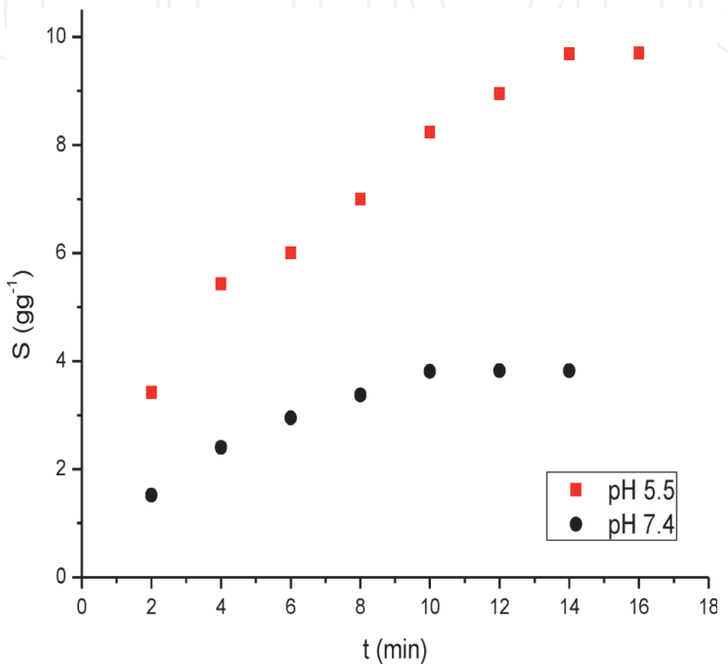

Figure 1.
Effect of two different pH mediums on the swelling kinetics of PEG/GG@AgNPs.

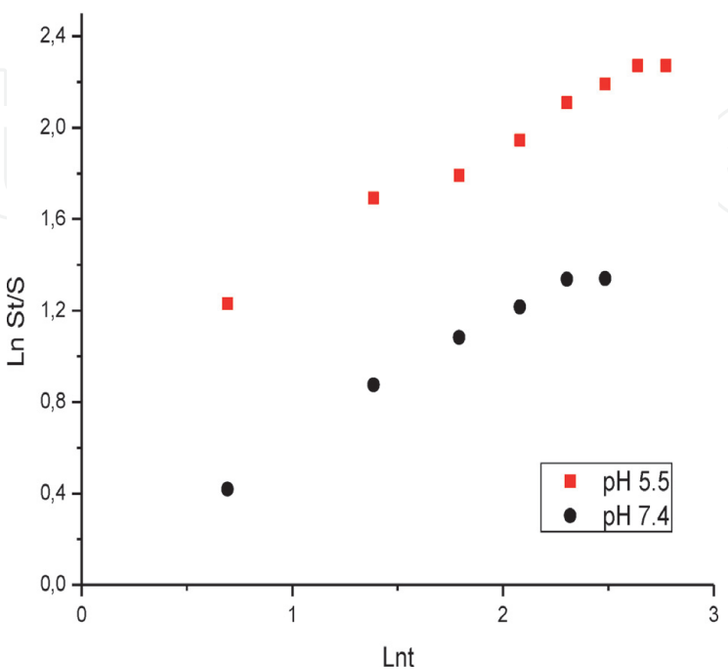

Figure 2.
Plots of Fickian kinetic model for PEG/GG@AgNPs.

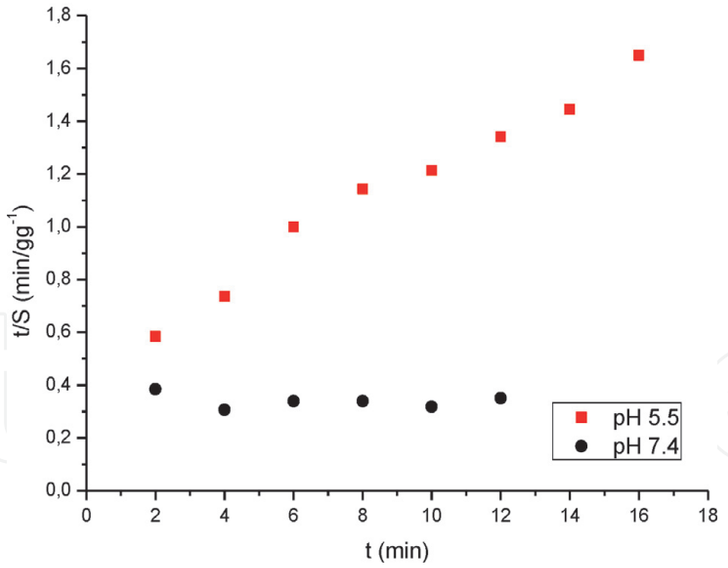

Figure 3.
Plots of Schott kinetic model for PEG/GG@AgNPs.

Sample	Fickian kinetic model			Schott kinetic model		
	n	k	R^2	$S_\infty(exp)$	k_2 (g/g min^{-1})	R^2
pH 5.5	0.51	2.50	0.987	1.39	1.052	0.978
pH 7.4	0.53	2.72	0.982	52.63	0.001	0.070

Table 1.
Values of various parameters associated with swelling kinetic models.

that it binds with O—H groups in the structure which allowed it to swell in a short time in pH 5.5. In order to explain swelling behavior of the nanoparticle, the swelling parameters were calculated by using the Fickian diffusion and Schott's second-order kinetic models. The calculated swelling kinetic parameters and the correlation coefficients (R^2) for all the models for the nanoparticles were given in **Table 1**.

The results showed that the linear equation of the Fickian diffusion kinetic model was best fit to explain the water diffusion mechanism of the nanoparticles with high correlation coefficient (R^2 = 0.982–0.987). According to the Fickian kinetic model, n is known to explain the diffusion mechanism of the solvent. The n values of the nanoparticles were calculated to be in the range of 0.5–1, which was explained by a non-Fickian diffusion behavior of the water transport mechanism [36].

3.2 STEM analysis

To investigate the effect of ultrasonic irradiation on the surface properties of the nanoparticle, the STEM images of PEG/GG@AgNPs were presented in **Figure 4**. It could be clearly seen that the surface of PEG was a homogeneous surface in spherical nanoform with the uniform dispersion of AgNPs. It was concluded that the ultrasonic irradiation may play a role in obtaining homogeneous distribution of the nanoparticles.

With this structural feature, nanoparticles have been used in different applications such as sensor, drug delivery system, and pharmaceutical applications [37–41].

Figure 4.
STEM image of PEG/GG@AgNPs.

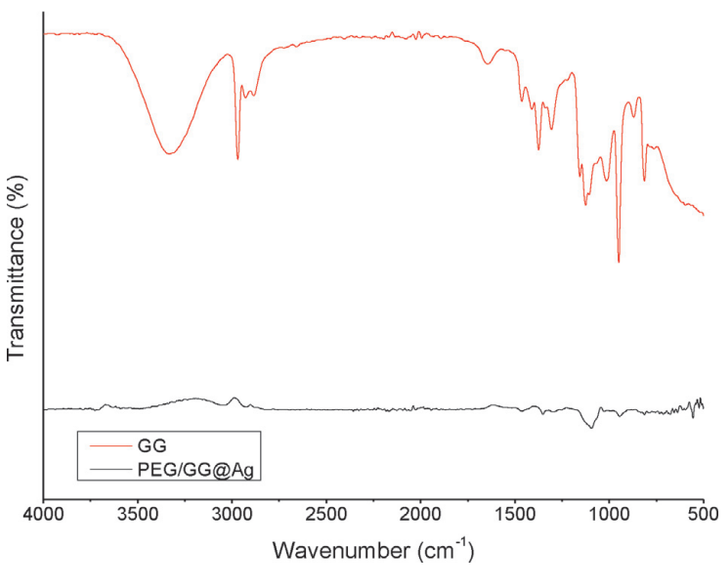

Figure 5.
The FTIR spectrums of pure GG and PEG/GG@AgNPs.

3.3 FTIR analysis

The FTIR spectrums of pure GG and PEG/GG@AgNPs were given in **Figure 5**. The FTIR spectrum of pure GG showed peaks at 3499 (—OH stretching), 2989 (C—H stretching), and 1030 (—OH bending) cm^{-1}. The FTIR spectrum of PEG/GG@AgNPs showed peaks at 2980 (C—H stretching), 1540 (COOH), 1470 (C—H stretching), and 1370 (—C=O) cm^{-1}. The peaks recorded at 3499 cm^{-1} of GG expressed in AgNPs indicated that -OH groups were utilized for the stabilization of AgNPs. From the results of the FTIR, we found that reduction and stabilization occurred in AgNPs. Singh et al. observed similar results [42].

4. Conclusions

In this study, PEG/GG@AgNPs were prepared by using sonochemical method. The swelling ability of nanoparticle was investigated in two different pHs. The

mechanism of swelling kinetics was explained, and it has been found that the mechanism follows the Fickian diffusion model. In summary, this study was focused on the green, low-cost novel method for producing Ag nanoparticles. The NPs could be served as a promising candidate nanocarrier for drug delivery systems due to its the swelling degrees.

Acknowledgements

The authors acknowledge the STEM and FTIR analysis support from ArelPOTKAM, Istanbul, and Zeynep Akça.

Author details

Selcan Karakus[1*], Ezgi Tan[1], Merve Ilgar[1], Ibrahim Mizan Kahyaoglu[1], Yeşim Müge Şahin[2,3], Demet Sezgin Mansuroglu[2,4], Deniz Ismik[2,5], Nevin Tasaltin[6] and Ayben Kilislioglu[1]

1 Faculty of Engineering, Department of Chemistry, Istanbul University-Cerrahpasa, Istanbul, Turkey

2 ArelPOTKAM (Polymer Technologies and Composite Application and Research Center), Istanbul Arel University, Istanbul, Turkey

3 Faculty of Engineering and Architecture, Department of Biomedical Engineering, Istanbul Arel University, Istanbul, Turkey

4 Department of Chemistry, Yildiz Technical University, Davutpasa Campus, Istanbul, Turkey

5 Faculty of Chemistry and Metallurgy, Department of Bioengineering, Yildiz Technical University, Istanbul, Turkey

6 Department of Electrical-Electronics Engineering, Maltepe University, Istanbul, Turkey

*Address all correspondence to: selcan@istanbul.edu.tr

References

[1] Bensaude-Vincent B. Building multidisciplinary research fields: The cases of materials science, nanotechnology and synthetic biology. In: The Local Configuration of New Research Fields. Cham: Springer; 2016. pp. 45-60

[2] Daniel MC, Astruc D. Gold nanoparticles: Assembly, supramolecular chemistry, quantum-size-related properties, and applications toward biology, catalysis, and nanotechnology. Chemical Reviews. 2004;**104**(1):293-346

[3] Abbasi E, Milani M, Fekri Aval S, Kouhi M, Akbarzadeh A, Tayefi Nasrabadi H, et al. Silver nanoparticles: Synthesis methods, bio-applications and properties. Critical Reviews in Microbiology. 2016;**42**(2):173-180

[4] Bang JH, Suslick KS. Applications of ultrasound to the synthesis of nanostructured materials. Advanced Materials. 2010;**22**(10): 1039-1059

[5] Wang ZL. Functional oxide nanobelts: Materials, properties and potential applications in nanosystems and biotechnology. Annual Review of Physical Chemistry. 2004;**55**: 159-196

[6] Scott BJ, Wirnsberger G, Stucky GD. Mesoporous and mesostructured materials for optical applications. Chemistry of Materials. 2001;**13**(10): 3140-3150

[7] Yin Y, Talapin D. The chemistry of functional nanomaterials. Chemical Society Reviews. 2013;**42**(7):2484-2487

[8] Sun X. Morphology and size-controllable preparation of silver nanostructures through a wet-chemical route at room temperature. Inorganic Materials. 2010;**46**(6):679-682

[9] Rosi NL, Mirkin CA. Nanostructures in biodiagnostics. Chemical Reviews. 2005;**105**(4):1547-1562

[10] Wu W, He Q, Jiang C. Magnetic iron oxide nanoparticles: Synthesis and surface functionalization strategies. Nanoscale Research Letters. 2008; **3**(11):397

[11] Eastman JA, Choi SUS, Li S, Yu W, Thompson LJ. Anomalously increased effective thermal conductivities of ethylene glycol-based nanofluids containing copper nanoparticles. Applied Physics Letters. 2001;**78**(6): 718-720

[12] Rai M, Yadav A, Gade A. Silver nanoparticles as a new generation of antimicrobials. Biotechnology Advances. 2009;**27**(1):76-83

[13] Hasan A, Waibhaw G, Saxena V, Pandey LM. Nano-biocomposite scaffolds of chitosan, carboxymethyl cellulose and silver nanoparticle modified cellulose nanowhiskers for bone tissue engineering applications. International Journal of Biological Macromolecules. 2018;**111**:923-934

[14] Abdullah MF, Ghosh SK, Basu S, Mukherjee A. Cationic guar gum orchestrated environmental synthesis for silver nano-bio-composite films. Carbohydrate Polymers. 2015;**134**:30-37

[15] Nair LS, Laurencin CT. Biodegradable polymers as biomaterials. Progress in Polymer Science. 2007;**32**(8-9):762-798

[16] Kumar T, Gupta SK, Prajapati MK, Tripathi D. Natural excipients: A review. Asian Journal of Pharmacy and Life Science. 2012;**2**(1):97-108. ISSN 2231–4423

[17] Anal AK. Bionanotechnology: Principles and Applications. USA: CRC Press; 2018

[18] Makshakova ON, Faizullin DA, Zuev YuF. Interplay between secondary structure and ion binding upon thermoreversible gelation of κ-carrageenan. Carbohydrate Polymers. 2020;**227**:115342

[19] Tiwari P, Panthari P, Katare DP, Kharkwal H. Natural polymers in drug delivery. World Journal of Pharmaceutical Sciences. 2014;**3**(9): 1395-1409

[20] Mudgil D, Barak S, Khatkar BS. Guar gum: Processing, properties and food applications—A review. Journal of Food Science and Technology. 2014; **51**(3):409-418

[21] Jani GK, Shah DP, Prajapati VD, Jain VC. Gums and mucilages: Versatile excipients for pharmaceutical formulations. Asian Journal of Pharmaceutical Sciences. 2009;**4**(5): 309-323

[22] Parente ME, Ochoa Andrade A, Ares G, Russo F, Jiménez-Kairuz Á. Bioadhesive hydrogels for cosmetic applications. International Journal of Cosmetic Science. 2015;**37**(5):511-518

[23] Kanmani P, Rhim JW. Physicochemical properties of gelatin/ silver nanoparticle antimicrobial composite films. Food Chemistry. 2014; **148**:162-169

[24] Palem RR, Madhusudana Rao K, Kang TJ. Self-healable and dual-functional guar gum-grafted-polyacrylamidoglycolic acid-based hydrogels with nano-silver for wound dressings. Carbohydrate Polymers. 2019;**223**:115074

[25] Shameli K, Bin Ahmad M, Jazayeri SD, Sedaghat S, Shabanzadeh P, Jahangirian H, et al. Synthesis and characterization of polyethylene glycol mediated silver nanoparticles by the green method. International Journal of Molecular Sciences. 2012;**13**(6):6639-6650

[26] Kora AJ, Sashidhar RB, Arunachalam J. Gum kondagogu (Cochlospermum gossypium): A template for the green synthesis and stabilization of silver nanoparticles with antibacterial application. Carbohydrate Polymers. 2010;**82**(3):670-679

[27] He C, Liu L, Fang Z, Li J, Guo J, Wei J. Formation and characterization of silver nanoparticles in aqueous solution via ultrasonic irradiation. Ultrasonics Sonochemistry. 2014;**21**(2): 542-548

[28] Wang Y, Xiong Y, Wang J, Zhang X. Ultrasonic-assisted fabrication of montmorillonite-lignin hybrid hydrogel: Highly efficient swelling behaviors and super-sorbent for dye removal from wastewater. Colloids and Surfaces A: Physicochemical and Engineering Aspects. 2017;**520**:903-913

[29] Wang X, Hou H, Li Y, Wang Y, Hao C, Ge C. A novel semi-IPN hydrogel: Preparation, swelling properties and adsorption studies of Co (II). Journal of Industrial and Engineering Chemistry. 2016;**41**:82-90

[30] Gharekhani H, Olad A, Mirmohseni A, Bybordi A. Superabsorbent hydrogel made of NaAlg-g-poly (AA-co-AAm) and rice husk ash: Synthesis, characterization, and swelling kinetic studies. Carbohydrate Polymers. 2017;**168**:1-13

[31] Wang M, Xu L, Ju X, Peng J, Zhai M, Li J, et al. Enhanced radiation crosslinking of carboxymethylated chitosan in the presence of acids or polyfunctional monomers. Polymer Degradation and Stability. 2008;**93**(10):1807-1813

[32] Vuković JS, Babić MM, Antić KM, Miljković MG, Perić-Grujić AA, Filipović JM, et al. A high efficacy antimicrobial acrylate based hydrogels with incorporated copper for wound healing application. Materials Chemistry and Physics. 2015;**164**:51-62

[33] Tanc B, Orakdogen N. Charged groups synergically enhanced elasticity and tunable swelling/shrinking of poly (dialkylaminoethyl methacrylate)/ layered silicate nanocomposite cryogels. Polymer. 2019;**178**:121627

[34] Lee JN, Park C, Whitesides GM. Solvent compatibility of poly (dimethylsiloxane)-based microfluidic devices. Analytical Chemistry. 2003; **75**(23):6544-6554

[35] Jamalabadi M, Saremnezhad S, Bahrami A, Jafari SM. The influence of bath and probe sonication on the physicochemical and microstructural properties of wheat starch. Food Science & Nutrition. 2019;**7**(7):2427-2435

[36] Dai H, Zhang H, Ma L, Zhou H, Yu Y, Guo T, et al. Green pH/magnetic sensitive hydrogels based on pineapple peel cellulose and polyvinyl alcohol: Synthesis, characterization and naringin prolonged release. Carbohydrate Polymers. 2019;**209**:51-61

[37] Slowing II, Trewyn BG, Giri S, Lin VY. Mesoporous silica nanoparticles for drug delivery and biosensing applications. Advanced Functional Materials. 2007;**17**(8):1225-1236

[38] West JL, Halas NJ. Engineered nanomaterials for biophotonics applications: Improving sensing, imaging, and therapeutics. Annual Review of Biomedical Engineering. 2003;**5**(1):285-292

[39] Soomro RA, Kalwar NH, Avci A, Pehlivan E, Hallam KR, Willander M. In-situ growth of NiWO4 saw-blade-like nanostructures and their application in photo-electrochemical (PEC) immunosensor systems designed for the detection of neuron-specific enolase. Biosensors and Bioelectronics. 2019;**141**: 111331

[40] Tunesi MM, Kalwar NH, Soomro RA, Karakus S, Jawaid S, Abro MI. Tartaric acid assisted in-situ growth of CuO nanostructures over ITO substrate for the electrocatalytic detection of Sudan I. Materials Science in Semiconductor Processing. 2018;**75**: 296-300

[41] Tunesi MM, Kalwar N, Abbas MW, Karakus S, Soomro RA, Kilislioglu A, et al. Functionalised CuO nanostructures for the detection of organophosphorus pesticides: A non-enzymatic inhibition approach coupled with nano-scale electrode engineering to improve electrode sensitivity. Sensors and Actuators B: Chemical. 2018;**260**: 480-489

[42] Singh J, Dhaliwal AS. Synthesis, characterization and swelling behavior of silver nanoparticles containing superabsorbent based on grafted copolymer of polyacrylic acid/Guar gum. Vacuum. 2018;**157**:51-60